

Emergent Cooperative Driving Strategies for Stop-and-Go Wave Mitigation via Multi-Agent Reinforcement Learning

Raphael Korbmacher¹, Daniel Straub², Antoine Tordeux¹, and Claudia Totzeck¹

¹University of Wuppertal, 42119 Wuppertal, Germany

²Technical University of Munich (TUM), 80333 Munich, Germany

Abstract

Stop-and-go waves in traffic flow pose a persistent challenge, compromising safety, efficiency, and environmental sustainability. This paper introduces a novel mitigation strategy discovered through training multi-agent deep reinforcement learning (DRL) agents in a simulated ring-road environment. The agents autonomously develop a cooperative driving policy, where most vehicles maintain minimal headways to maximize throughput, while a single “buffer” vehicle adopts a larger headway to absorb perturbations and prevent wave propagation. This strategy enhances stability without sacrificing overall flow. We further demonstrate that adapting this cooperative strategy to classical car-following models, such as the Intelligent Driver Model (IDM), yields improved stability and traffic efficiency. Furthermore, we show within a parametrised linear framework that the cooperative strategy can optimise system performance under stability constraints. Our findings offer promising insights for future autonomous vehicle systems and highway management.

Keywords—Stop-and-go waves, traffic stability, multi-agent reinforcement learning, cooperative driving, Intelligent Driver Model

1 Introduction

Traffic jams represent an undesirable traffic condition with numerous negative consequences, including economic losses, increased fuel consumption, and higher pollutant emissions [1, 2]. Causes of traffic jams can include bottlenecks, accidents, or construction sites, but can also arise for no apparent reason. These spontaneous jams are often referred to as phantom jams or, in this context, stop-and-go waves (SGW). Despite more than seven decades of research into stop-and-go dynamics, the emergence of self-sustaining waves in traffic flow remains incompletely understood.

The focus of this paper is on identifying strategies to prevent or mitigate the emergence of SGWs. Beyond strategic planning measures such as variable speed limits [3, 4], the prevention of stop-and-go traffic has been approached from two main perspectives. The first is a microscopic one, which examines the behavior of individual vehicles to determine if it can reduce or eliminate stop-and-go waves. These approaches are known as Jam-Absorption Driving (JAD) strategies. The second perspective is collective, termed traffic string stability analysis, where traffic is considered unstable if perturbations amplify along the flow.

Although there are anecdotal reports of individuals mitigating stop-and-go waves through their driving behavior [5], JAD was not scientifically investigated until 2013 by Nishi et al. [1]. Two common JAD strategies that can foster SGW suppression are the “slow-in” and “fast-out” approach, as well as maintaining a large time gap between subsequent vehicles to avoid deceleration until the stop phase of the SGW has passed [6]. Ideally, this allows the vehicle to hold and guide all following vehicles to approach an upcoming wave in a controlled manner, thereby achieving SGW suppression [7]. However, these strategies are controversial and give rise to a *first paradox*: while maintaining a high time gap may reduce SGWs in specific instances, if all vehicles adopt this strategy, it reduces overall traffic efficiency and outflow.

The macroscopic perspective of analyzing traffic stability has a longer history, beginning with the first car-following models in the 1950s, with pioneering contributions from Reuschel [11] and Pipes [12]. The question of traffic stability and SGWs inherent to delayed first-order and second-order models soon emerged and remains under investigation today (see, e.g., the review [13]). In Fig. 1, the top panel shows the speed-time profile of an unstable traffic situation

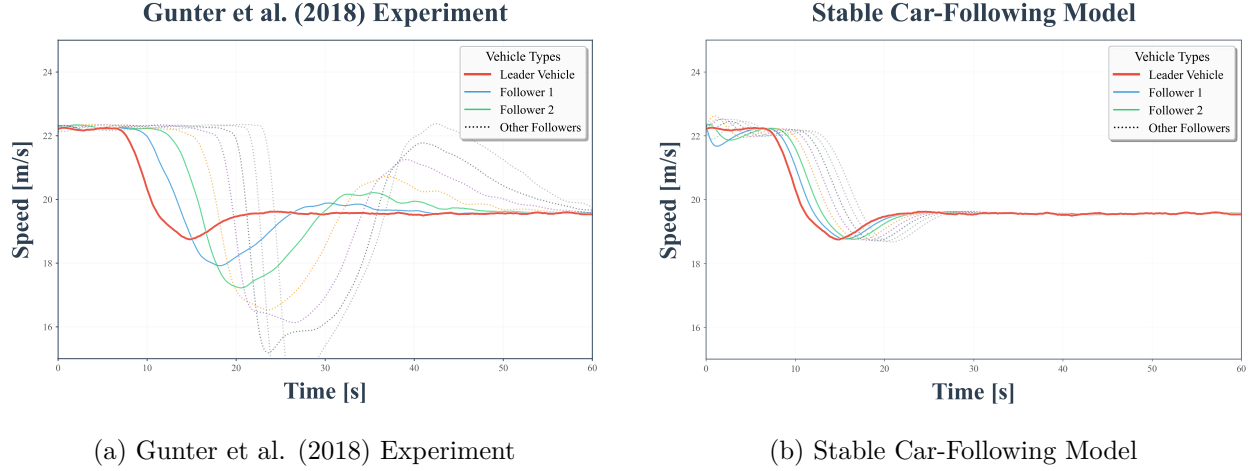


Figure 1: Speed profiles of an eight-vehicle platoon. Upper panel: an unstable platoon observed experimentally [8]. Lower panel: a simulated platoon using a stable CTG car-following model [9] where perturbations are overdamped. The trajectories can be computed and visualized online; see [10].

from the experiments of Gunter et al. [8]. The bottom panel depicts the speed-time profile of a stable traffic situation simulated using the Constant Time Gap (CTG) model [9].

Following years of theoretical investigations on the stability of traffic using car-following models [14–16], the analysis of stability in real traffic situations with human drivers began with Sugiyama et al. (2008) [17] and their famous circuit road experiment. Their study demonstrated how a uniform flow of 22 vehicles on a closed-loop track could spontaneously transition into a traffic jam due to small fluctuations in driver behavior, even without bottlenecks or external disruptions. Similar experiments reaching the same conclusions have been conducted by [18–20]. These studies show that human driving behavior is inherently unstable, leading to stop-and-go traffic without obvious causes. Consequently, expectations that technological solutions such as Adaptive Cruise Control (ACC) and autonomous vehicles can improve traffic stability rose [21–24]. While initial expectations were high, and experiments like Stern et al. (2018) [20] showed positive effects of autonomous vehicles on traffic stability, subsequent works have revealed that current market technologies are even more unstable than human drivers [8, 25–27]. This leads to the *second paradox*: manufacturers must balance stable behavior against comfort, often prioritizing the latter (individual incentives over collective ones) [24]. Although technologically not yet realized, researchers agree that vehicle-to-vehicle communication will have a positive impact on mitigating SGW [28–30]. This relates to so-called Cooperative ACC (CACC) systems, in which vehicles are connected and communicate with each other. These communications can significantly reduce the system response times, by eliminating the need for external sensors, which are prone to delays [31]. They can also enable vehicles to cooperate, for example by synchronising emergency braking or facilitating manoeuvres such as cutting in and out [32, 33]. Inter-vehicle cooperation could also mitigate SGW formation by assigning specific roles to each vehicle.

In this contribution, we train Deep Reinforcement Learning (DRL) agents in an experimental setup similar to Sugiyama's experiment. Through this, we discover a cooperative strategy that resolves both paradoxes. Rather than homogeneous traffic, where all vehicles behave in the same way, the DRL agents exhibit heterogeneous behaviour. One vehicle acts as a *buffer*, maintaining a large time gap, while the others follow closely behind, as in a *platoon*. Through simulations with a car following model, we verify that this cooperative strategy indeed improves stability and traffic flow. Furthermore, we demonstrate within a parametrised linear framework, that the cooperative strategy optimises system performance under stability constraints. Although implementation in the real world is not yet realistic, we envision this as the future of highway traffic.

2 Deep Reinforcement Learning

In this chapter, we introduce DRL as applied to the car-following problem. DRL extends traditional reinforcement learning (RL) by incorporating deep neural networks to handle high-dimensional state spaces, enabling more effective learning in complex environments such as vehicle control [34]. The RL and DLR approaches are currently being developed extensively to mitigate stop-and-go waves [35–39]. We first outline the foundational concepts of RL and DRL, tailored to our car-following scenario, before detailing the specific setup, training configurations, and observations.

Reinforcement learning is a machine learning paradigm that aims to maximize the discounted cumulative rewards over a finite horizon in a Markov Decision Process (MDP). This MDP is formally defined by the tuple $\mathcal{P} = (\mathcal{S}, \mathcal{A}, \mathcal{T}, \mathcal{R}, \mathcal{T}_0, \gamma)$, where \mathcal{S} denotes the set of states; \mathcal{A} represents the set of possible actions; $\mathcal{T} : \mathcal{S} \times \mathcal{A} \times \mathcal{S} \rightarrow [0, 1]$ is the transition function specifying the probability of transitioning to state s' from state s given action a ; $\mathcal{R} : \mathcal{S} \times \mathcal{A} \times \mathcal{S} \rightarrow \mathbb{R}$ is the reward function; $\mathcal{T}_0 : \mathcal{S} \rightarrow [0, 1]$ is the initial state distribution; and $\gamma \in (0, 1]$ is the discount factor for future rewards [40]. An initial state $s_0 \sim \mathcal{T}_0$ is sampled. The agent, modeled as a policy $\pi_\theta(a|s)$ parameterized by θ , selects an action $a_0 \sim \pi_\theta(\cdot|s_0)$. This leads to a new state $s_1 \sim \mathcal{T}(\cdot|s_0, a_0)$ and reward $r_0 = \mathcal{R}(s_0, a_0, s_1)$. The process repeats until termination, generating a trajectory $\tau = (s_i, a_i, r_i)_{i \geq 0}$ [41]. DRL builds upon this framework by using deep neural networks to describe the policy π_θ or approximate value functions, allowing the agent to learn from raw, high-dimensional inputs.

2.1 Experimental setup

The car-following problem is modeled as a one-dimensional longitudinal control scenario where each vehicle (agent) must follow the preceding vehicle safely, stably, and comfortably while maintaining a desired speed and mitigating SGWs [42]. To simulate a realistic dense multi-vehicle traffic situation, we adopt a ring road topology inspired by the Sugiyama experiment [17], implemented using the Gymnasium framework [43]. The road is a circular loop of 220 meters in length, populated with 15 to 25 vehicles, creating a high-density scenario prone to traffic oscillations. Each vehicle is modeled as an agent in a multi-agent environment. For scalable training, we apply a shared policy across all agents and use a single-agent DRL algorithm for policy updates, treating experiences from individual agents independently while they interact within the shared simulation. At each time step t with simulation timestep $\delta t = 0.1$ s, the DRL agent observes a four-dimensional state vector: its own velocity v_t , the relative distance to the front vehicle d_t , the relative velocity to the front vehicle Δv_t , and the front vehicle's velocity $v_{t,f}$. Including $v_{t,f}$ provides redundant but potentially stabilizing information to the neural network. The action space is continuous, consisting of a single acceleration command $a_t \in [-5, 2] \text{ m/s}^2$, as per ISO 15622 standards for adaptive cruise control systems [44]. For policy approximation, we utilize Proximal Policy Optimization (PPO) [45], selected for its sample efficiency and stability in continuous control tasks. The policy network is a multi-layer perceptron (MLP) with three hidden layers of 64 units each, using ReLU activations. Hyperparameters include a learning rate of 3×10^{-4} , discount factor $\gamma = 0.99$, GAE lambda of 0.95, clip range of 0.2, entropy coefficient of 0.01, and value function coefficient of 0.5, tuned empirically for convergence. More informations are accesible at https://github.com/RaphaelVZU/DRL_Vehicle_SGW_Experiment.

2.2 Training

A crucial aspect of the DRL approach is the design of a reward function that balances multiple objectives: safety, efficiency, comfort, and stability. In our experiments, for each vehicle in the DRL model, the reward r_t at time t is defined as:

$$r(t) = w_v r_v(t) + w_d r_d(t) + w_s r_s(t), \quad (1)$$

where the velocity reward $r_v(t) = -|v(t) - v_d|/v_d$ penalizes deviation from the desired velocity $v_d = 10 \text{ m/s}$, the distance reward $r_d(t) = -|d(t) - d^*(t)|/d^*(t)$ encourages maintaining the desired headway $d^*(t) = T v(t) + \ell$, with $T > 0$ the time gap parameter and $\ell > 0$ the minimum spacing, while the safety reward $r_s(t)$ employs a zone-based approach that provides bonuses for safe spacing and increasingly severe penalties for unsafe proximity.

To enhance robustness, we introduce perturbations during training: random emergency braking events applied to random vehicles with probability 0.03 per step, lasting up to 30 steps (3 s) at 80% of maximum deceleration (-4 m/s^2). In addition, Gaussian noise ($\mathcal{N}(0, 0.5) \text{ m}$) is added to distance measurements to simulate sensor inaccuracies. We trained each agent's policy for 200,000 timesteps, using a batch size of 64 [46].

2.3 Emergent cooperative strategy

After the training we evaluate the models by observing the achieved mean speed, the mitigation of SGWs, and the robustness against perturbations. Surprisingly, the agents did not exhibit uniform behavior but instead developed a cooperative strategy that enhanced traffic stability and robustness against perturbations. This strategy is illustrated in Fig. 2, where 22 DRL agents navigate a circular road with periodic boundary conditions.

In conventional car-following models, all vehicles adhere to the same governing equations, resulting in uniform behavior. In contrast, our DRL agents exhibited non-uniform behavior, with one vehicle maintaining a large gap to the preceding vehicle. We refer to this vehicle as the “buffer vehicle.” This represents a cooperative strategy that emerges only if the buffer vehicle suppresses the incentive to close the gap, thereby stabilizing the entire traffic flow. Furthermore, the other vehicles must also cooperate by maintaining small time gaps to the vehicle in front. If other vehicles also increased their time gaps, this strategy would lose its efficiency, which is why altering the behavior of only the buffer vehicle is insufficient.

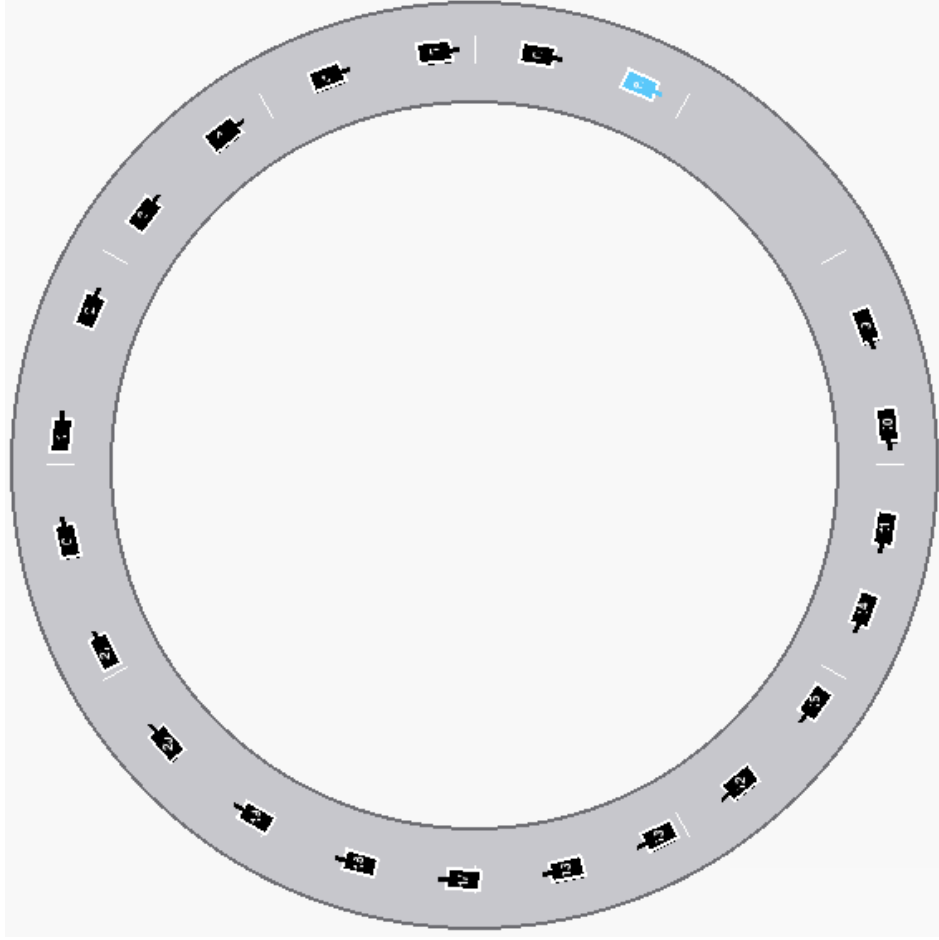


Figure 2: Typical observation of the multi-agent DRL. The headway distances of almost all vehicles are close to the safety-critical time gap. Only one vehicle (cyan) maintains a very large headway.

3 Model-based Validation of the Cooperative Strategy

In this chapter, we show that the cooperative buffering strategy found with the DRL approach has a positive impact on mean velocity and stability of the traffic. To this end, we implement this strategy in classical car-following models. Whereas the DRL agents are trained with thousands of parameters (the weights of the neural network) that cannot be directly interpreted, car-following models are transparent with only a few parameters. Therefore, the models are well suited to examine the effect of the strategy under otherwise identical conditions.

3.1 Intelligent Driver car-following model

For our investigations, we employ the Intelligent Driver Model (IDM) proposed by Treiber et al. [47]. The IDM is a second-order car-following model in which the position $x_n(t)$ and velocity $v_n(t)$ of the n -th vehicle at time t evolve according to the dynamics:

$$\frac{dx_n(t)}{dt} = v_n(t), \quad (2)$$

while

$$\frac{dv_n(t)}{dt} = a \left[1 - \left(\frac{g(v_n(t), v_{n+1}(t))}{d_n(t) - \ell} \right)^2 - \left(\frac{v_n(t)}{v_{\max}} \right)^4 \right], \quad (3)$$

where $d_n(t) = x_{n+1}(t) - x_n(t)$ is the distance to the leading vehicle ($n+1$), $\ell \geq 0$ is the vehicle length, v_{\max} is the maximum speed, $a > 0$ is the maximum acceleration, and $g(v_n, v_{n+1})$ is the desired gap given by

$$g(v_n, v_{n+1}) = g_0 + v_n T - \frac{v_n(v_{n+1} - v_n)}{2\sqrt{ab}}, \quad (4)$$

where $g_0 \geq 0$ is the minimum gap, $T > 0$ is the desired time gap, and $b > 0$ is the comfortable deceleration.

3.2 Simulation results

For our experiments, we use a ring road topology with $N = 20$ vehicles on a circular road of length 201 meters, similar to the DRL setup, to induce dense traffic conditions prone to SGWs. The parameters are set as follows: $a = 1 \text{ m/s}^2$, $b = 2 \text{ m/s}^2$, $v_{\max} = 20 \text{ m/s}$, $\ell = 5 \text{ m}$, $g_0 = 1 \text{ m}$ and nominal time gap $T = 1 \text{ s}$. Such parameter setting makes the uniform solution linearly unstable in the non-cooperative case, where the time gap for each vehicle is equal to the nominal time gap. Simulations are performed with a time step of $dt = 0.01 \text{ s}$ using an explicit-implicit Euler scheme, which is implicit for position updates and explicit for speed updates. The initial condition corresponds to a traffic jam in which the gap between vehicles is equal to the minimum gap of one meter.

The left panels of Fig. 3 show the results for the classical IDM, where all vehicles use the same parameters, including $T = 1 \text{ s}$. Fig. 3(a) displays the vehicle trajectories, revealing the emergence of persistent SGW that propagate backward. The corresponding speed profiles in Fig. 3(b) confirm the instability, with large oscillations in velocity that are highest at the beginning, due to the jam initial positions, fall until 60 seconds of simulations and then slightly start to rise again before being stationary. This leads to reduced average speed (approximately 3.66 m/s) and potentially increased fuel consumption due to frequent accelerations and decelerations.

To implement the buffering strategy, we introduce a parameter $B \geq 1$ which is a scaling factor for the buffer vehicle with an enlarged time gap

$$T_{\text{buf}} = BT. \quad (5)$$

For the remaining $N - 1$ vehicles, the time gap is set by

$$T_{\text{platoon}} = T \frac{N - B}{N - 1}. \quad (6)$$

So, the average time gap

$$\bar{T} = \frac{1}{N} [(N - 1)T_{\text{platoon}} + T_{\text{buf}}] = T$$

is equal to the nominal time gap T , i.e., the equilibrium mean speeds of the cooperative and non-cooperative systems are the same. In addition, the case $B = 1$ corresponds to the non-cooperative strategy where the time gap for each vehicle is equal to the nominal time gap.

The right panels of Fig. 3 illustrate the results with $B = 7$, so $T_{\text{buf}} = 4 \text{ s}$ and $T_{\text{platoon}} \approx 0.84 \text{ s}$ for the others. Fig. 3(c) shows the trajectories, where the perturbations are absorbed, preventing the formation of sustained SGWs. The speed profiles in Fig. 3(d) oscillating heavy at the beginning, but get smoother after some time. The average speed is around 4.06 m/s.

The simulation results of Fig. 3 demonstrate that the cooperative buffering strategy enables flow stability by maintaining system performance for the IDM car-following model. We find that the choice of car-following model appears to be irrelevant. Additional simulation results, which are not reported here, show that the strategy provides stability and performance improvements also for other car-following models, such as the *optimal velocity model* [49] or the full velocity difference model [50].

In the next section, we formalize the SGW suppression as an optimization problem and show that the cooperative strategy outperforms the non-cooperative one in terms of maximizing flow under stability constraints.

4 Model-based strategy optimization

In this section, using a general linearised car-following model we demonstrate that the single-vehicle buffering strategy maximises the mean vehicle speed while ensuring stability, clearly outperforming the non-cooperative strategy.

4.1 Optimal stability control problem

Consider N vehicles on a one-dimensional segment of length L with periodic boundaries, and the general linear car-following model

$$\frac{d}{dt} v_n(t) = a_n d_n(t) + b_n v_n(t) + c_n v_{n+1}(t), \quad (7)$$

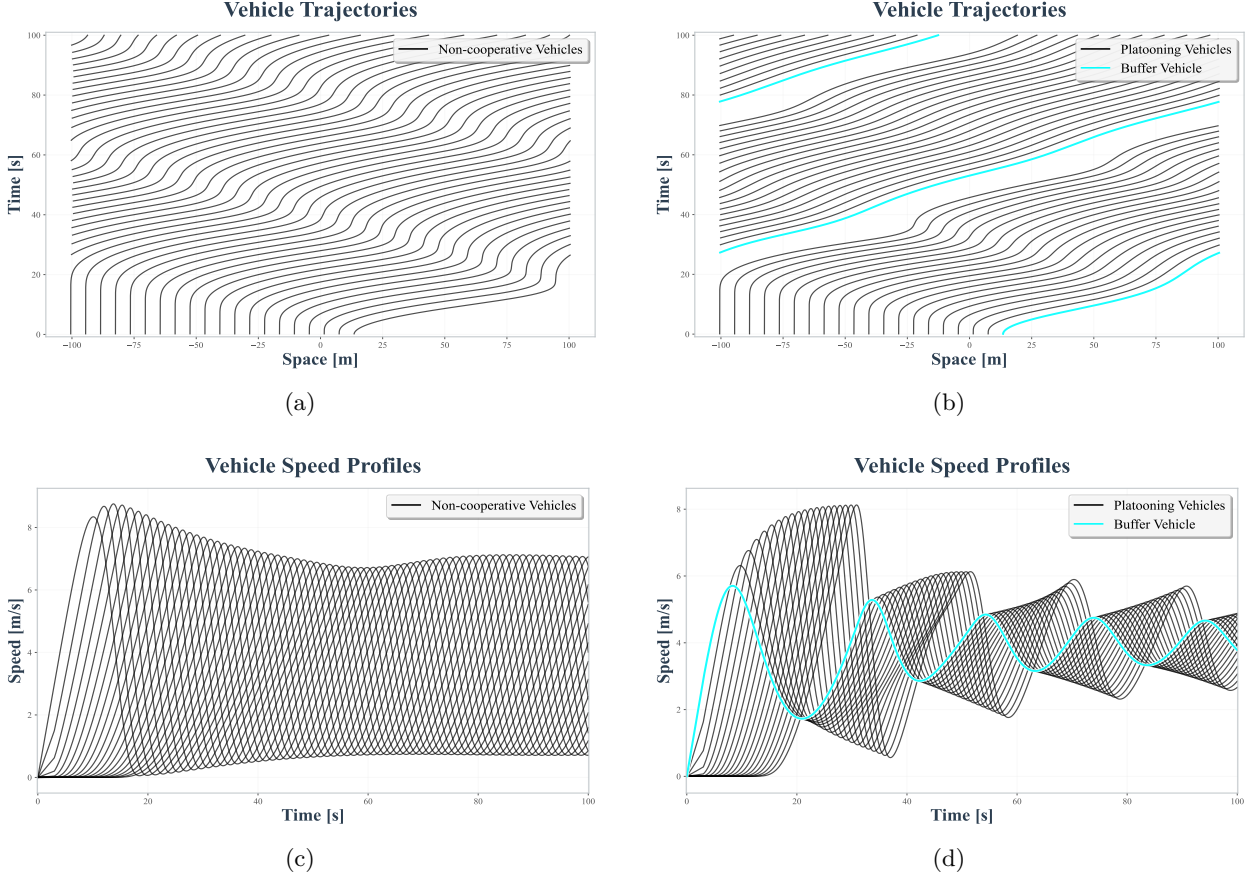


Figure 3: Simulation results using identical IDM parameter settings, without (left panels) and with (right panels) the buffering cooperative strategy. Both scenarios start from the same initial traffic jam condition. Top row: vehicle trajectories; bottom row: corresponding speed profiles. Without the strategy (left) a stop-and-go wave emerges and propagates upstream. With the buffering cooperative strategy (right) the traffic flow converges to homogeneous laminar flow. The trajectories can be computed and visualized online; see [48].

where $v_n(t) = \frac{d}{dt}x_n(t)$, $d_n(t) = x_{n+1}(t) - x_n(t)$, $a_n > 0$, $b_n < 0$, and $c_n \geq 0$ for all $n \in \{1, \dots, N\}$. The uniform equilibrium solution corresponds to the state where all vehicles move with the same velocity v and maintain spacing d_n , such that their accelerations are zero; that is, $a_n d_n + b_n v + c_n v = 0$ for all $n \in \{1, \dots, N\}$. This uniform solution is stable if [51]

$$\sum_{n=1}^N \frac{b_n^2 - c_n^2}{2a_n^2} \geq \sum_{n=1}^N \frac{1}{a_n}. \quad (8)$$

We have $c_n = 0$ for all $n \in \{1, \dots, N\}$ since we do not consider the speed of the leader in the reward function. In addition, the cost term $|d_n - T_n v_n - \ell|$ implies $b_n = a_n T_n$. The stability condition then becomes

$$\sum_{n=1}^N T_n^2 \geq \sum_{n=1}^N \frac{2}{a_n} =: \alpha > 0, \quad (9)$$

where (T_1, \dots, T_N) are the time gap parameters.

The equilibrium solution $((d_1, \dots, d_N), v)$ of the car-following model is such that

$$d_n = v T_n + \ell, \quad \text{for all } n \in \{1, \dots, N\}.$$

The sum of the distances is conserved on the periodic system:

$$\sum_{n=1}^N d_n(t) = L, \quad \text{for all } t \geq 0.$$

Thus, the equilibrium speed satisfies

$$\sum_{n=1}^N [vT_n + \ell] = L,$$

which simplifies to

$$v(T_1, \dots, T_N) = \frac{\tilde{L}}{\sum_{n=1}^N T_n}, \quad (10)$$

where $\tilde{L} = L - N\ell$.

In summary, the optimal stability control problem is to maximise the mean speed, which following (10) is equivalent to minimising the sum of the time gaps

$$\text{Minimise} \quad \sum_{n=1}^N T_n, \quad (11)$$

subject to the stability constraint (9)

$$\sum_{n=1}^N T_n^2 \geq \alpha, \quad (12)$$

and the lower bound constraint on the time gaps

$$T_1, \dots, T_N \geq T_{\min} > 0. \quad (13)$$

We furthermore suppose that

$$\alpha \geq NT_{\min}^2, \quad (14)$$

which holds, for instance, if $T_{\min} \leq \min_n \sqrt{2/a_n}$.

4.2 Non-cooperative optimal solution

First, we investigate the optimality of the non-cooperative strategy, in which all vehicles maintain the same time gap. The Lagrangian of the optimisation problem reads

$$\mathcal{L} = \sum_{n=1}^N (T_n + \mu_n(T_{\min} - T_n)) - \lambda \left(\sum_{n=1}^N T_n^2 - \alpha \right),$$

where λ is the Lagrange multiplier for the stability constraint and μ_n are the multipliers for the time gap constraints with $n = 1, \dots, N$, respectively. First-order optimality conditions are given by

$$\begin{aligned} 1 - \mu_n - 2\lambda T_n &= 0, & \alpha - \sum_{n=1}^N T_n^2 &\leq 0, \\ T_{\min} - T_n &\leq 0, & \lambda \geq 0, & \mu_n \geq 0, \quad \text{for all } n \in \{1, \dots, N\}. \end{aligned}$$

Rewriting the first equation we obtain

$$T_n = \frac{\mu_n - 1}{-2\lambda} \quad \text{for all } n \in \{1, \dots, N\}.$$

Since $T_{\min} > 0$ and $\lambda \geq 0$, this yields the condition $\mu_n \in (0, 1)$ for each $n \in \{1, \dots, N\}$.

Assuming a non-cooperative strategy, each agent tries to minimize their time gap individually, which leads to $\mu_n = \mu_m$ for all $n, m \in \{1, \dots, N\}$, i.e., any stationary point has all components equal, $T_n = T_{\text{non}}$. This together with minimization in (11) yields equality in the stability constraint and we obtain

$$T_{\text{non}} = \sqrt{\frac{\alpha}{N}}. \quad (15)$$

Hence, the Lagrange system yields the uniform solution $T_n = T_{\text{non}} = \sqrt{\alpha/N}$ for all $n \in \{1, \dots, N\}$. The corresponding mean speed reads

$$v_{\text{non}} = \frac{\tilde{L}}{\sqrt{N\alpha}}. \quad (16)$$

Note that the stability condition no longer holds for any smaller time gap where the mean speed would have been higher. Therefore, the uniform solution for which $T_n = \sqrt{\alpha/N}$ for all $n \in \{1, \dots, N\}$ is optimal, at least locally. In fact, this uniform solution is the optimal non-cooperative solution. However, as we will see in the next section, cooperative strategies can overcome this local optimum. More precisely, the buffering cooperative strategy enables the global optimum to be achieved.

4.3 Cooperative optimal solution

Choosing all μ_n equal (i.e. acting non-cooperatively) is just one way to satisfy the first-order optimality conditions. Based on the results from the DRL and the numerical simulations, we investigate a cooperative approach allowing for different time gaps in the following.

To this end, we assume that the time gaps admit the structure

$$T_n = T_{\min} + u_n, \quad u_n \geq 0 \text{ for all } n \in \{1, \dots, N\}.$$

Then

$$\sum_{n=1}^N T_n = NT_{\min} + s, \quad s = \sum_{n=1}^N u_n,$$

and

$$\sum_{n=1}^N T_n^2 = NT_{\min}^2 + 2T_{\min}s + \sum_{n=1}^N u_n^2.$$

Put $B = \alpha - NT_{\min}^2 > 0$, the stability constraint (12) becomes

$$\sum_{n=1}^N u_n^2 + 2T_{\min}s \geq B.$$

Then, remarking that $s^2 = \sum_{n=1}^N u_n^2 + \sum_{n \neq m} u_n u_m \geq \sum_{n=1}^N u_n^2$ as the u_n are positive, we obtain the inequality

$$\sum_{n=1}^N u_n^2 \leq \left(\sum_{n=1}^N u_n \right)^2 = s^2.$$

So any feasible s must satisfy $s^2 + 2T_{\min}s \geq B$. Computing the nonnegative root of the quadratic equation $s^2 + 2T_{\min}s = B$ yields

$$s^* = -T_{\min} + \sqrt{T_{\min}^2 + B} = -T_{\min} + \sqrt{\alpha - (N-1)T_{\min}^2}.$$

This lower bound on s is attainable because equality $\sum_{n=1}^N u_n^2 = s^2 = \left(\sum_{n=1}^N u_n \right)^2$ can be attained by concentrating all of s in a single coordinate (set one $u_{n_0} = s^*$, others $u_n = 0, n \neq n_0$). Therefore, under the assumption (4.3) the global minimiser is

$$\begin{cases} T_n^* = T_{\min}, & n \neq n_0, \\ T_{n_0}^* = T_{\min} + s^* = \sqrt{\alpha - (N-1)T_{\min}^2}, \end{cases} \quad (17)$$

where $n_0 \in \{1, \dots, N\}$. Hereby, it is straightforward to check that $T_{n_0}^* = \sqrt{\alpha - (N-1)T_{\min}^2} \geq \sqrt{\alpha/N} \geq T_{\min}$, from $\alpha \geq NT_{\min}^2$, while $T_n^* = T_{\min} \leq \sqrt{\alpha/N}$ (see (14)). Thus, we qualitatively recover the buffering cooperative strategy learned through reinforcement learning in Sec. 2 and validated by simulation in Sec. 3. The buffering vehicle is the one assigned a desired time gap of $T_{n_0}^*$. Note that there are N possible strategies, since any of the N vehicles can act as the buffering vehicle. In addition, the global optimum is achieved when only a single vehicle acts as a buffer, irrespective of the number of vehicles in the system. The reduced time gap between vehicles in the platoon is T_{\min} and is independent of N . However, the buffering time gap does depend on N . The larger the number of vehicles N , the larger the buffering time gap (in the form of a quadratic root function and up the limit $N \leq \alpha T_{\min}^2$, see (14)).

Finally, the optimal mean speed reads

$$v_{\text{coop}}^* = \frac{\tilde{L}}{(N-1)T_{\min} + \sqrt{\alpha - (N-1)T_{\min}^2}}. \quad (18)$$

Note that this global optimum is higher than the local optimal mean speed derived in (16). Indeed, using the Cauchy-Schwarz inequality for the nonnegative vector $T = (T_1, \dots, T_N)$ we obtain

$$\left(\sum_{n=1}^N T_n \right)^2 \leq N \sum_{n=1}^N T_n^2.$$

Since $\sum_{n=1}^N (T_n^*)^2 = \alpha$, this gives the upper bound

$$\sum_{n=1}^N T_n^* = (N-1)T_{\min} + \sqrt{\alpha - (N-1)T_{\min}^2} \leq \sqrt{N\alpha},$$

and

$$v_{\text{non}} \leq v_{\text{coop}}^*,$$

with equality if and only if $T_1 = \dots = T_N = T_{\text{non}} = \sqrt{\alpha/N}$, i.e., by recovering the non-cooperative optimum.

5 Conclusion and Outlook

In this paper, we explored strategies to mitigate stop-and-go waves in traffic flow, drawing from both deep reinforcement learning and classical car-following models. Through training DRL agents in a ring road environment inspired by the Sugiyama experiment, we observed the emergence of a cooperative buffering strategy: one vehicle maintains a significantly larger time gap to act as a buffer, while the others follow closely. This approach not only stabilizes the traffic but also enhances overall flow efficiency, resolving the two paradoxes identified in the introduction. First, it avoids the efficiency loss associated with uniformly large time gaps by concentrating the buffering effort in a single vehicle. Second, it demonstrates that stability can be achieved without sacrificing comfort or individual incentives, as the strategy optimizes collective performance. To validate this, we implemented the buffering strategy in the IDM, showing through simulations that it suppresses SGWs, increases average speeds, and reduces oscillations compared to non-cooperative configurations. Furthermore, by formulating an optimization problem under linear stability constraints, we proved that this buffer approach leads to higher mean speed and overall traffic efficiency. These findings suggest that future traffic systems could benefit from cooperative behaviors, potentially enabled by connected and autonomous vehicles. This is especially promising for truck platoons, where the platooning vehicles can maintain the tight spacing required for substantial aerodynamic drag reduction, while the buffer vehicle preserves stability. Although current implementations face challenges like the need for vehicle-to-vehicle communication, our work provides a theoretical foundation for designing more resilient traffic control algorithms. Looking ahead, several avenues for extension warrant investigation. First, empirical validation through real-world experiments. Second, while our optimization proves that a single buffer vehicle is globally optimal, real-world conditions are more complex. Future work should therefore investigate multi-buffer strategies that adjust the number and position of buffer vehicles. Finally, exploring the economic and environmental impacts—such as reduced fuel consumption and emissions—could quantify the societal benefits, paving the way for policy recommendations in intelligent transportation systems.

Acknowledgment

The authors acknowledge the research project *SmartACC* funded in Germany by the Deutsche Forschungsgemeinschaft (DFG, German Research Foundation), grant number 546728715.

Contents

1	Introduction	1
2	Deep Reinforcement Learning	2
2.1	Experimental setup	3
2.2	Training	3
2.3	Emergent cooperative strategy	3
3	Model-based Validation of the Cooperative Strategy	4
3.1	Intelligent Driver car-following model	4
3.2	Simulation results	5

4 Model-based strategy optimization	5
4.1 Optimal stability control problem	5
4.2 Non-cooperative optimal solution	7
4.3 Cooperative optimal solution	8
5 Conclusion and Outlook	9

References

- [1] R. Nishi, A. Tomoeda, K. Shimura, and K. Nishinari, “Theory of jam-absorption driving,” *Transportation Research Part B: Methodological*, vol. 50, pp. 116–129, 2013.
- [2] X. Li, J. Cui, S. An, and M. Parsafard, “Stop-and-go traffic analysis: Theoretical properties, environmental impacts and oscillation mitigation,” *Transportation Research Part B: Methodological*, vol. 70, pp. 319–339, 2014.
- [3] A. Hegyi, B. De Schutter, and J. Hellendoorn, “Optimal coordination of variable speed limits to suppress shock waves,” *IEEE Transactions on intelligent transportation systems*, vol. 6, no. 1, pp. 102–112, 2005.
- [4] A. Hegyi and S. P. Hoogendoorn, “Dynamic speed limit control to resolve shock waves on freeways-field test results of the specialist algorithm,” in *13th International IEEE Conference on Intelligent Transportation Systems*. IEEE, 2010, pp. 519–524.
- [5] W. Beaty, “Traffic “experiments” and a cure for waves & jams,” <http://trafficwaves.org/trafexp.html>, accessed: 2025-10-08.
- [6] S. Wang, Z. Li, Z. Cao, A. Jolfaei, and Q. Cao, “Jam-absorption driving strategy for improving safety near oscillations in a connected vehicle environment considering consequential jams,” *IEEE Intelligent Transportation Systems Magazine*, vol. 14, no. 2, pp. 41–52, 2021.
- [7] Z. He, J. Laval, Y. Han, A. Hegyi, R. Nishi, and C. Wu, “A review of stop-and-go traffic wave suppression strategies: Variable speed limit vs. jam-absorption driving,” *arXiv preprint arXiv:2504.11372*, 2025.
- [8] G. Gunter, D. Gloudemans, R. E. Stern, S. McQuade, R. Bhadani, M. Bunting, M. L. Delle Monache, R. Lysecky, B. Seibold, J. Sprinkle *et al.*, “Are commercially implemented adaptive cruise control systems string stable?” *IEEE Transactions on Intelligent Transportation Systems*, vol. 22, no. 11, pp. 6992–7003, 2020.
- [9] J. Zhou and H. Peng, “String stability conditions of adaptive cruise control algorithms,” *IFAC Proceedings Volumes*, vol. 37, no. 22, pp. 649–654, 2004.
- [10] “Online simulation modul: Damped stability versus overdamped stability,” https://www.vzu.uni-wuppertal.de/fileadmin/site/vzu/Damped_stability_VS_Overdamped_stability.html?speed=0.5, accessed: 2025-10-08.
- [11] A. Reuschel, “Vehicle movements in a platoon,” *Oesterreichisches Ingenieur-Archiv*, vol. 4, pp. 193–215, 1950.
- [12] L. A. Pipes, “An operational analysis of traffic dynamics,” *Journal of applied physics*, vol. 24, no. 3, pp. 274–281, 1953.
- [13] R. E. Wilson and J. A. Ward, “Car-following models: fifty years of linear stability analysis—a mathematical perspective,” *Transportation Planning and Technology*, vol. 34, no. 1, pp. 3–18, 2011.
- [14] G. Orosz, R. Wilson, and G. Stépán, “Traffic jams: dynamics and control,” pp. 4455–4479, 2010.
- [15] I. Gasser, G. Siritto, and B. Werner, “Bifurcation analysis of a class of ‘car following’ traffic models,” *Physica D: Nonlinear Phenomena*, vol. 197, no. 3-4, pp. 222–241, 2004.
- [16] G. Orosz, R. Wilson, and B. Krauskopf, “Global bifurcation investigation of an optimal velocity traffic model with driver reaction time,” *Physical Review E*, vol. 70, no. 2, p. 026207, 2004.
- [17] Y. Sugiyama, M. Fukui, M. Kikuchi, K. Hasebe, A. Nakayama, K. Nishinari, S.-i. Tadaki, and S. Yukawa, “Traffic jams without bottlenecks—experimental evidence for the physical mechanism of the formation of a jam,” *New journal of physics*, vol. 10, no. 3, p. 033001, 2008.

[18] S.-i. Tadaki, M. Kikuchi, M. Fukui, A. Nakayama, K. Nishinari, A. Shibata, Y. Sugiyama, T. Yosida, and S. Yukawa, "Phase transition in traffic jam experiment on a circuit," *New Journal of Physics*, vol. 15, no. 10, p. 103034, 2013.

[19] R. Jiang, M.-B. Hu, H. Zhang, Z.-Y. Gao, B. Jia, Q.-S. Wu, B. Wang, and M. Yang, "Traffic experiment reveals the nature of car-following," *PloS one*, vol. 9, no. 4, p. e94351, 2014.

[20] R. E. Stern, S. Cui, M. L. Delle Monache, R. Bhadani, M. Bunting, M. Churchill, N. Hamilton, H. Pohlmann, F. Wu, B. Piccoli *et al.*, "Dissipation of stop-and-go waves via control of autonomous vehicles: Field experiments," *Transportation Research Part C: Emerging Technologies*, vol. 89, pp. 205–221, 2018.

[21] M. Treiber and D. Helbing, "Microsimulations of freeway traffic including control measures," *at - Automatisierungstechnik*, vol. 49, no. 11, p. 478, 2001.

[22] L. Davis, "Effect of adaptive cruise control systems on traffic flow," *Physical Review E*, vol. 69, no. 6, p. 066110, 2004.

[23] A. Bose and P. Ioannou, "Analysis of traffic flow with mixed manual and intelligent cruise control vehicles: Theory and experiments," California Partners for Advanced Transit and Highways, Tech. Rep., 2001.

[24] R. Korbmacher, P. Khound, and A. Tordeux, "Understanding collective stability of ACC systems: From theory to real-world observations," *arXiv preprint arXiv:2504.04530*, 2025.

[25] M. Makridis, K. Mattas, D. Borio, R. Giuliani, and B. Ciuffo, "Estimating reaction time in adaptive cruise control system," in *2018 IEEE intelligent vehicles symposium (IV)*. IEEE, 2018, pp. 1312–1317.

[26] M. Makridis, K. Mattas, B. Ciuffo, F. Re, A. Kriston, F. Minarini, and G. Rognelund, "Empirical study on the properties of adaptive cruise control systems and their impact on traffic flow and string stability," *Transportation research record*, vol. 2674, no. 4, pp. 471–484, 2020.

[27] B. Ciuffo, K. Mattas, M. Makridis, G. Albano, A. Anesiadou, Y. He, S. Josvai, D. Komnos, M. Pataki, S. Vass *et al.*, "Requiem on the positive effects of commercial adaptive cruise control on motorway traffic and recommendations for future automated driving systems," *Transportation Research Part C: Emerging Technologies*, vol. 130, p. 103305, 2021.

[28] D. De Bruin, J. Kroon, R. Van Klaveren, and M. Nelisse, "Design and test of a cooperative adaptive cruise control system," in *IEEE Intelligent Vehicles Symposium, 2004*. IEEE, 2004, pp. 392–396.

[29] F. Bu, H.-S. Tan, and J. Huang, "Design and field testing of a cooperative adaptive cruise control system," in *Proceedings of the 2010 American Control Conference*. IEEE, 2010, pp. 4616–4621.

[30] V. Milanés, S. E. Shladover, J. Spring, C. Nowakowski, H. Kawazoe, and M. Nakamura, "Cooperative adaptive cruise control in real traffic situations," *IEEE Transactions on intelligent transportation systems*, vol. 15, no. 1, pp. 296–305, 2013.

[31] J. S. Brunner, M. A. Makridis, and A. Kouvelas, "Comparing the observable response times of ACC and CACC systems," *IEEE Transactions on Intelligent Transportation Systems*, vol. 23, no. 10, pp. 19 299–19 308, 2022.

[32] G. Arnaout and S. Bowling, "Towards reducing traffic congestion using cooperative adaptive cruise control on a freeway with a ramp," *Journal of Industrial Engineering and Management (JIEM)*, vol. 4, no. 4, pp. 699–717, 2011.

[33] D. Kapsalis, J. Spring, and X.-Y. Lu, "Cooperative handling of cut-ins and emergency braking for connected automated vehicles with heterogeneous powertrains," 2025.

[34] V. Francois-Lavet, P. Henderson, R. Islam, M. G. Bellemare, J. Pineau *et al.*, "An introduction to deep reinforcement learning," *Foundations and Trends® in Machine Learning*, vol. 11, no. 3-4, pp. 219–354, 2018.

[35] A. R. Kreidieh, C. Wu, and A. M. Bayen, "Dissipating stop-and-go waves in closed and open networks via deep reinforcement learning," in *2018 21st international conference on intelligent transportation systems (itsc)*. IEEE, 2018, pp. 1475–1480.

[36] M. Li, Z. Li, C. Xu, and T. Liu, "Deep reinforcement learning-based vehicle driving strategy to reduce crash risks in traffic oscillations," *Transportation research record*, vol. 2674, no. 10, pp. 42–54, 2020.

[37] L. Jiang, Y. Xie, X. Wen, D. Chen, T. Li, and N. G. Evans, “Dampen the stop-and-go traffic with connected and automated vehicles—a deep reinforcement learning approach,” in *2021 7th International Conference on Models and Technologies for Intelligent Transportation Systems (MT-ITS)*. IEEE, 2021, pp. 1–6.

[38] A. Richardson, X. Wang, A. Dubey, and J. Sprinkle, “Reinforcement learning with communication latency with application to stop-and-go wave dissipation,” in *2024 IEEE Intelligent Vehicles Symposium (IV)*. IEEE, 2024, pp. 1187–1193.

[39] K. Jang, N. Lichtle, E. Vinitsky, A. Shah, M. Bunting, M. Nice, B. Piccoli, B. Seibold, D. B. Work, M. L. Delle Monache *et al.*, “Reinforcement learning-based oscillation dampening: Scaling up single-agent reinforcement learning algorithms to a 100-autonomous-vehicle highway field operational test,” *IEEE Control Systems*, vol. 45, no. 1, pp. 61–94, 2025.

[40] M. Lapan, *Deep reinforcement learning hands-on*. Packt Publishing Birmingham, 2018, vol. 6.

[41] P. Ladosz, L. Weng, M. Kim, and H. Oh, “Exploration in deep reinforcement learning: A survey,” *Information Fusion*, vol. 85, pp. 1–22, 2022.

[42] F. Hart, O. Okhrin, and M. Treiber, “Towards robust car-following based on deep reinforcement learning,” *Transportation research part C: emerging technologies*, vol. 159, p. 104486, 2024.

[43] M. Towers, A. Kwiatkowski, J. Terry, J. U. Balis, G. De Cola, T. Deleu, M. Goulão, A. Kallinteris, M. Krimmel, A. KG *et al.*, “Gymnasium: A standard interface for reinforcement learning environments,” *arXiv preprint arXiv:2407.17032*, 2024.

[44] *Intelligent transport systems - Adaptive Cruise Control systems — Performance requirements and test procedures, 2nd Edition*, International Organization for Standardization (ISO) Std. ISO 15 622, Apr. 2018.

[45] J. Schulman, F. Wolski, P. Dhariwal, A. Radford, and O. Klimov, “Proximal policy optimization algorithms,” *arXiv preprint arXiv:1707.06347*, 2017.

[46] R. Korbacher, “Code of the DRL experiment in github,” https://github.com/RaphaelVZU/DRL_Vehicle_SGW_Experiment, 2025, accessed: 2025-11-12.

[47] M. Treiber, A. Hennecke, and D. Helbing, “Congested traffic states in empirical observations and microscopic simulations,” *Physical Review E*, vol. 62, no. 2, p. 1805, 2000.

[48] “Online simulation modul: Stop-and-go mitigation via cooperative buffering,” https://www.vzu.uni-wuppertal.de/fileadmin/site/vzu/Stop-and-Go_Mitigation_via_Cooperative_Buffering.html?speed=0.4, accessed: 2025-11-03.

[49] M. Bando, K. Hasebe, A. Nakayama, A. Shibata, and Y. Sugiyama, “Dynamical model of traffic congestion and numerical simulation,” *Physical review E*, vol. 51, no. 2, p. 1035, 1995.

[50] R. Jiang, Q. Wu, and Z. Zhu, “Full velocity difference model for a car-following theory,” *Physical Review E*, vol. 64, no. 1, p. 017101, 2001.

[51] D. Ngoduy, “Effect of the car-following combinations on the instability of heterogeneous traffic flow,” *Transportmetrica B: transport dynamics*, vol. 3, no. 1, pp. 44–58, 2015.